INL/JOU-21-64091-Revision-0

Seeing through nuclear fuel: Three-dimensional, nondestructive X-ray microscopy and volumetric analyses of neutron-irradiated TRISO-coated fuel kernels

Changing the World's Energy Future

Nikolaus Cordes, William C Chuirazzi, Joshua J Kane, John D Stempien

Idaho National Laboratory

INL/JOU-21-64091-Revision-0

Seeing through nuclear fuel: Three-dimensional, nondestructive X-ray microscopy and volumetric analyses of neutron-irradiated TRISO-coated fuel kernels

Nikolaus Cordes, William C Chuirazzi, Joshua J Kane, John D Stempien

December 2021

Idaho National Laboratory
Idaho Falls, Idaho 83415

http://www.inl.gov

Prepared for the
U.S. Department of Energy
Under DOE Idaho Operations Office
Contract DE-AC07-05ID14517

Seeing through nuclear fuel: Three-dimensional, nondestructive X-ray microscopy and volumetric analyses of neutron-irradiated TRISO-coated fuel kernels

Nikolaus L. Cordes[1*], William C. Chuirazzi[1], Joshua J. Kane[1], and John D. Stempien[2]

[1]Characterization and Advanced Post-Irradiation Examinations Division, Idaho National Laboratory, Idaho Falls, ID

[2]Nuclear Fuels and Materials Division, Idaho National Laboratory, Idaho Falls, ID

*corresponding author, email: nikolaus.cordes@inl.gov

Abstract

The three-dimensional (3D) characterization of nuclear fuel with X-ray microscopy has historically proven difficult, due to uranium's high attenuation of easily accessible X-rays, both in a laboratory setting and at a synchrotron user facility. However, this imaging modality provides nondestructive information that can be used to investigate morphological changes arising from external stimuli (e.g., neutron irradiation, high temperature testing, etc.). By using an appropriate X-ray energy spectrum and an adequate X-ray filter, suitable transmissions through properly sized nuclear fuel specimens can be achieved. Here, we present the methods and results of using a commercially available, laboratory-based X-ray microscope (XRM) to examine the extent of 3D morphological changes of tristructural isotropic (TRISO)-coated fuel particles, specifically uranium oxide/uranium carbide fuel kernels, after high-temperature neutron irradiation.

Introduction

Uranium-bearing coated particle fuels, used in high-temperature gas-cooled reactors, have been in development since the 1960's and are widely studied in terms of their form, fabrication, performance, safety, and failure mechanisms [1, 2]. Typical TRISO fuels are a coated particle design comprised of either a UO_2 or UCO (i.e., a heterogeneous mixture of uranium oxide and uranium carbide) spherical kernel enveloped by four coating layers intended to retain fission products during irradiation and provide structural stability. The innermost coating is a low-density pyrolytic carbon layer (i.e., buffer layer, designed to provide void space for fission product gases), with the next layer being comprised of a high-density inner pyrolytic carbon (IPyC) layer. A silicon carbide (SiC) layer provides structural integrity and is a physical barrier to prevent non-gaseous fission product release. The outer pyrolytic carbon (OPyC) layer is designed as a final gaseous fission product barrier. Several thousand TRISO particles are consolidated into a graphitic and carbonized resin matrix to form a lager fuel element (e.g., cylinders or spheres). While many variations in TRISO-based fuel designs exist, the interested reader is referred to a review by Demkowicz et al. for further information [2].

To assess TRISO fuel performance after irradiation testing, characterizations are conducted to investigate morphological evolution of the fuel kernel and coating layers. Fuel kernel swelling, porosity, fracture, and migration, in addition to coating layer fracture and separation, are of interest to gauge the performance of the fuel under both nominal and off-normal conditions. Typical post-irradiation microstructural characterization techniques include electron microscopy and ceramography [3-5]. However, these techniques require destructive sample preparation and are inherently limited to two-dimensional (2D) cross-sectional imaging.

In contrast, micro X-ray computed tomography (micro-XCT) is a nondestructive 3D surface/bulk imaging technique applicable to the characterization of a wide variety of materials [6]. Typically, several hundred to several thousand X-radiographs are acquired as a function of sample rotation then mathematically reconstructed to a 3D dataset (i.e., tomogram). The contrast is based on X-ray photon attenuation and transmission of the sample material. In recent years, advances in micro-focus laboratory-based XRMs have enabled researchers to use this modality for robust 3D materials characterizations with the micro-XCT imaging technique [7].

Several studies have employed micro-XCT to image unirradiated or neutron-irradiated TRISO particles bearing surrogate (e.g., Al_2O_3) or fuel (i.e., uranium)-based kernels. Due to the high mass attenuation coefficient of uranium (relative to the typical X-ray energies available with common X-ray tube sources or synchrotron sources), these studies have been limited to characterization of surrogate kernels and surrounding coating layers or, in the case of fuel-bearing particles, only the coating layers [8-15].

Here, we report the use of micro-XCT to image and assess UCO fuel kernels contained within three irradiated TRISO particles using a laboratory-based XRM. By using an appropriate X-ray energy spectrum and adequate X-ray beam filter, tomograms of the fuel kernels were produced and quantitatively analyzed with volumetric digital image analysis tools.

Materials and methods

The TRISO particles in this study were irradiated at Idaho National Laboratory's Advanced Test Reactor during the second series of test irradiations for the Advanced Gas Reactor (AGR) Fuel Development and Qualification Program (these tests are referred to as AGR-2) [16]. Detailed information of the particles is provided in Section S1 of supplementary information (SI).

Micro-XCT was performed using a ZEISS Xradia 520 Versa XRM (Carl Zeiss X-ray Microscopy Inc., Dublin, CA). Detailed experimental methods are provided in SI, Section S2 and Figures S1 and S2.

Results and discussion

By imaging with X-ray energies below uranium's K absorption edge (~115.6 keV) and filtering unnecessary low X-ray energies (otherwise attenuated by the kernel), X-ray transmission of ~20% through the UCO fuel kernel was achieved (see SI, Fig. S3). This was sufficient for high quality tomographic reconstructions. A 2D reconstructed cross-sectional image of the center of Particle 1 is presented in Fig. 1a and 1b at two separate grayscale ranges. Within the low grayscale value range (Fig. 1a), the TRISO particle's coating layers (buffer, IPyC, and SiC) are observed. The regions corresponding to the fuel kernel are displayed as white pixels, as these actual values are outside of the display range in the figure. While the signal-to-noise ratio of the coating layers is considerably low (see SI, Fig. S3), a radial gap can be

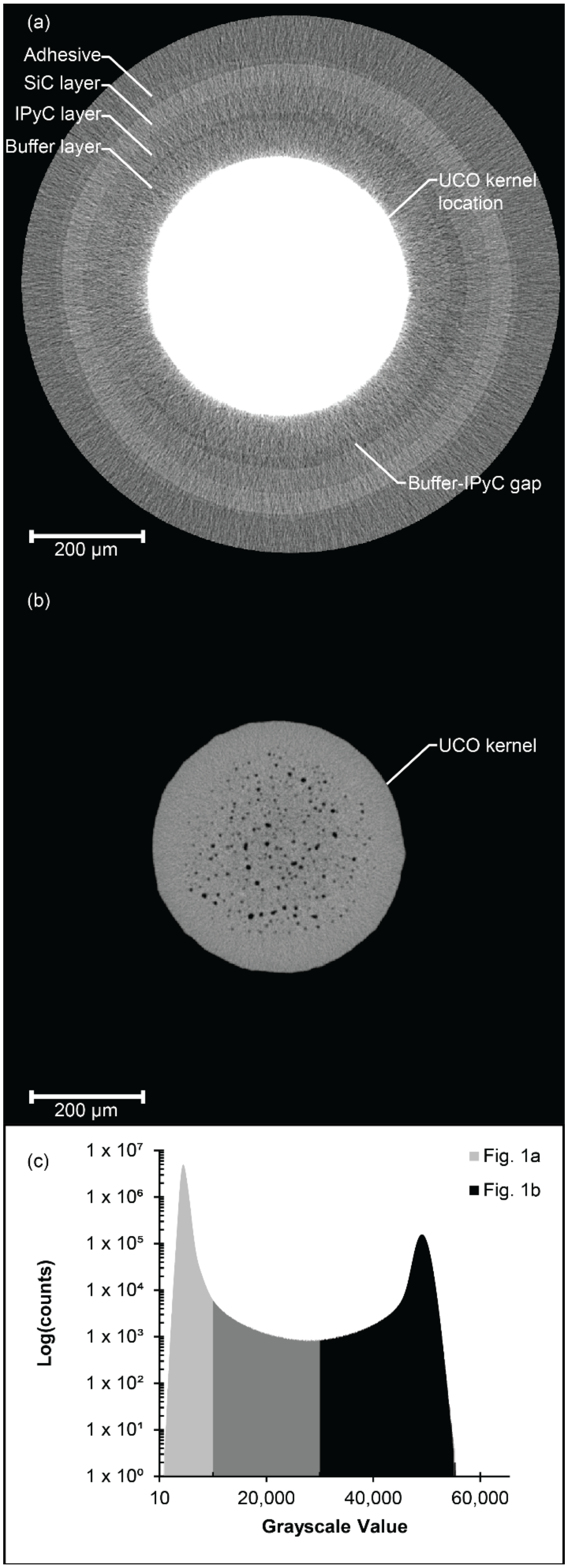

Fig. 1 Reconstructed 2D horizontal cross-sectional (i.e., slice) images of Particle 1, taken from the center of the particle. The displayed grayscale value range is adjusted to 0 – 10000 **a** to observe the TRISO coatings. **b** Details in the fuel kernel are observed by shifting the displayed grayscale value range to 30000-65535. **c** A histogram of the grayscale values of the tomogram (binned with a value of 10 grayscale values), with values colored in light gray and black corresponding to the ranges used for **a** and **b**, respectively. Counts corresponding to a grayscale value of 0 have been omitted from the histogram for clarity

observed between the buffer and IPyC layers (Fig. 1a), consistent with findings by Bower et al. and Rice et al. in the post-irradiation ceramography of AGR-1 and AGR-2 particles, respectively [4, 5]. The lack of complete debonding of the buffer layer from the IPyC layer is noted and observed for Particles 2 and 3 (see SI, Fig. S4). No IPyC or SiC cracking or SiC failure precursors (e.g., thinning from fission product attack) are observed in the tomograms [17].

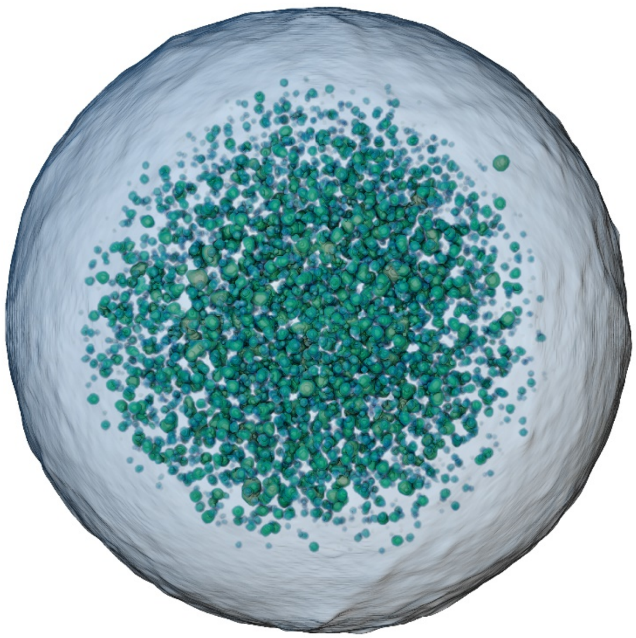

Fig. 2 A transparent rendering of the outer surface of an irradiated UCO fuel kernel (Particle 1) and volume rendering of internal voids (rendered with cubic interpolation)

Adjusting the grayscale range to higher values allows for the observation of the fuel kernel (Fig. 1b), revealing internal voids formed by the generation of fission gases (primarily krypton and xenon) during irradiation which contribute to kernel swelling [4]. Voids are also observed for Particles 2 and 3 (see SI, Fig. S5). By segmenting the fuel kernel and voids (details provided in SI, Section S2 and Figs. S1, S2), 3D visualizations were produced, as shown in the rendering displayed in Fig. 2.

Table 1. Measurements of UCO kernels and voids from segmented tomograms for each TRISO particle

	Sample		
Kernel Measurement	Particle 1	Particle 2	Particle 3
Kernel volume (mm^3)	4.922×10^{-2}	4.954×10^{-2}	5.208×10^{-2}
Kernel volume increase (%)[a]	22.5	23.5	29.6
Kernel ESD (μm)	454.6	455.7	463.3
Kernel sphericity[b]	0.991	0.975	0.974
Void Measurement			
Number of voids (n_v)	6112	4924	7407
Number of voxels rejected from ESD calculation (n_r)[c]	314	291	429
Total void volume (mm^3)	7.654×10^{-4}	4.731×10^{-4}	6.530×10^{-4}
Kernel porosity (%)	1.555	0.955	1.254
Mean void ESD (μm)[d]	5.48 ± 2.21	5.08 ± 1.98	4.96 ± 1.88
Mean void distance from center (μm)[b]	121.1 ± 34.41	126.3 ± 31.99	126.6 ± 33.31

[a]Calculated using the experimentally determined kernel volume and the calculated spherical volume from nominal kernel diameter of 425 μm.
[b]See SI, Section S1 for sphericity calculation details.
[c]Voids with volumes less than 3 voxels were discarded from mean void ESD calculations (see SI, Section S4) [18-22].
[d]Uncertainties are the standard deviations of the means.

The segmented voxels corresponding to the UCO kernel and voids were used to calculate the kernel volume increase (i.e., kernel swelling) that is observed in irradiated TRISO particles (Table 1). The kernel swellings range from 22.5% for Particle 1 to 29.6% for Particle 3 and are consistent with swelling of 30% ± 14% reported by Stempien et al. in the analysis of 97 AGR-2 TRISO particles using serial ceramography [23]. Other measurements include kernel equivalent spherical diameter (ESD) and kernel sphericity (Table 1).

Quantitative analyses were also carried out for each kernel's voids. The number of voids (n_v) *detected* vary significantly with each particle. Kernel porosities range from 0.954% (Particle 2) to 1.554% (Particle 1). Void ESDs were averaged (Table 1), with a considerable difference noted between Particles 1 and 3. Histograms for each particle are provided in SI, Fig. S6. Student's t-tests were performed for the mean void ESD of each particle pair (see SI, Tables S2-S4), and indicate the ESD of each particle is statistically different at a 95% confidence level [24].

Void geometric distances from kernel centers were calculated and averaged for each particle (see SI, Section S2) and range from 121.1 µm for Particle 1 to 126.3 µm for Particle 3 (Table 1). Histograms for each particle are provided in SI, Fig. S7. The results of Student's t-tests (see SI, Tables S5-7) indicate that the average void distances for Particles 2 and 3 are statistically similar at the 95% confidence level, while the average void distance for Particle 1 is statistically different.

Individual void ESDs plotted as a function of distance from kernel center provides a view of a stochastic void distribution (see SI, Fig. S8). To better visualize this information, voids were grouped into 10 µm-diameter spheres and the mean void ESDs for each particle were plotted as a function of the mean distance of the grouped void populations from the kernel center (see SI, Fig. S9). The mean void ESDs for Particle 1 are largest near the kernel center and gradually decrease toward the kernel edge whereas the trends for Particles 2 and 3 exhibit a gradual increase in mean void ESD to a peak near 150 µm from the kernel center with a rapid decrease thereafter.

Using these 3D measurements, observations of particle similarities and differences can be made. Namely, n_v of Particle 3 is significantly larger than that observed for Particles 1 and 2, leading to increased kernel swelling despite Particle 3's relatively low mean void ESD. Interestingly, the kernel porosity and mean void ESD for Particle 1 are the largest in the group, while exhibiting the lowest kernel swelling and the highest sphericity. These differences may be attributed to a difference in each particle's thermal history during AGR-2: the average calculated daily temperature difference of TRISO Compact 6-4-1 was ~200 °C, with a peak of 321 °C.

Conclusions

We have reported methods and results of imaging irradiated TRISO-coated fuel particles, with an emphasis on the volumetric analyses of UCO fuel kernels and internal voids. The nondestructive 3D imaging methods presented here provides kernel volumetric data acquired in reasonable imaging times (~8 h per particle). These methods can be useful to the nuclear energy scientific community by providing valuable information on 3D fuel kernel morphology evolution during irradiation. For example, thermomechanical TRISO fuel models, such as the PARticle FUel ModEl (PARFUME), currently utilize a kernel swelling parameter derived from UO_2 fuel

[25]. Measurements of UCO kernel swelling via laboratory-based XRM could expand the UCO database and improve these models' predictive capabilities.

Acknowledgements

The authors acknowledge Drs. Aaron Craft and Paul Demkowicz for helpful discussions, Mr. Miles Cook for assistance in sample handling and preparation, and the Irradiated Materials Characterization Laboratory facility staff for operational support.

Funding

This work was sponsored by the U.S. Department of Energy, Office of Nuclear Energy, through the Advanced Reactor Technologies Advanced Gas Reactor Fuel Development and Qualification Program. Idaho National Laboratory is operated by Battelle Energy Alliance LLC under contract number DE-AC07-05ID14517 for the U.S. Department of Energy.

Declarations

Conflicts of interest

The authors declare no conflict of interest.

References

1. M.S.T. Price: The Dragon Project origins, achievements and legacies *Nuclear Engineering and Design.* **251**, 60 (2012).
2. P.A. Demkowicz, B. Liu and J.D. Hunn: Coated particle fuel: Historical perspectives and current progress *Journal of Nuclear Materials.* **515**, 434 (2019).
3. I.J. van Rooyen, D.E. Janney, B.D. Miller, P.A. Demkowicz and J. Riesterer: Electron microscopic evaluation and fission product identification of irradiated TRISO coated particles from the AGR-1 experiment: A preliminary review *Nuclear Engineering and Design.* **271**, 114 (2014).
4. G.R. Bower, S.A. Ploger, P.A. Demkowicz and J.D. Hunn: Measurement of kernel swelling and buffer densification in irradiated UCO-TRISO particles *Journal of Nuclear Materials.* **486**, 339 (2017).
5. F.J. Rice, J.D. Stempien and P.A. Demkowicz: Ceramography of irradiated TRISO fuel from the AGR-2 experiment *Nuclear Engineering and Design.* **329**, 73 (2018).
6. E. Maire and P.J. Withers: Quantitative X-ray tomography *International Materials Reviews.* **59**(1), 1 (2014).
7. A.P. Merkle and J. Gelb: The Ascent of 3D X-ray Microscopy in the Laboratory *Microscopy Today.* **21**(2), 10 (2013).
8. C.A. Baldwin, J.D. Hunn, R.N. Morris, F.C. Montgomery, C.M. Silva and P.A. Demkowicz: First elevated-temperature performance testing of coated particle fuel compacts from the AGR-1 irradiation experiment *Nuclear Engineering and Design.* **271**, 131 (2014).
9. T. Lowe, R.S. Bradley, S. Yue, K. Barii, J. Gelb, N. Rohbeck, J. Turner and P.J. Withers: Microstructural analysis of TRISO particles using multi-scale X-ray computed tomography *Journal of Nuclear Materials.* **461**, 29 (2015).
10. C.M. Silva, L.L. Snead, J.D. Hunn, E.D. Specht, K.A. Terrani and Y. Katoh: Application of X-ray microcomputed tomography in the characterization of irradiated nuclear fuel and material specimens *J Microsc.* **260**(2), 163 (2015).

11. J.D. Hunn, C.A. Baldwin, F.C. Montgomery, T.J. Gerczak, R.N. Morris, G.W. Helmreich, P.A. Demkowicz, J.M. Harp and J.D. Stempien: Initial examination of fuel compacts and TRISO particles from the US AGR-2 irradiation test *Nuclear Engineering and Design.* **329**, 89 (2018).
12. R.N. Morris, J.D. Hunn, C.A. Baldwin, F.C. Montgomery, T.J. Gerczak and P.A. Demkowicz: Initial results from safety testing of US AGR-2 irradiation test fuel *Nuclear Engineering and Design.* **329**, 124 (2018).
13. L. Zhu, X. Xiang, Y. Peng and X. Wang: Three-Dimensional Measurement of TRISO Coated Particle Using Micro Computed Tomography *Science and Technology of Nuclear Installations.* **2019**, 2908538 (2019).
14. G.W. Helmreich, D. Richardson, S. Venkatakrishnan and A. Ziabari: Method for measurement of TRISO kernel and layer volumes by X-ray computed tomography *Journal of Nuclear Materials.* **539**, 152255 (2020).
15. D. Liu, S. Knol, J. Ell, H. Barnard, M. Davies, J.A. Vreeling and R.O. Ritchie: X-ray tomography study on the crushing strength and irradiation behaviour of dedicated tristructural isotropic nuclear fuel particles at 1000 °C *Materials & Design.* **187**, 108382 (2020).
16. P.A. Demkowicz, B.P. Collin, D.A. Petti, G.L. Hawkes, J.W. Sterbentz, B.T. Pham, D.M. Scates and D.E. Stacey: Results of the AGR-2 TRISO fuel performance demonstration irradiation experiment in the Advanced Test Reactor *Annals of Nuclear Energy.* **150**, 107833 (2021).
17. D.A. Petti, J. Buongiorno, J.T. Maki, R.R. Hobbins and G.K. Miller: Key differences in the fabrication, irradiation and high temperature accident testing of US and German TRISO-coated particle fuel, and their implications on fuel performance *Nuclear Engineering and Design.* **222**(2), 281 (2003).
18. H. Nyquist: Certain Topics in Telegraph Transmission Theory *Transactions of the American Institute of Electrical Engineers.* **47**(2), 617 (1928).
19. C.E. Shannon: Communication in the Presence of Noise *Proceedings of the IRE.* **37**(1), 10 (1949).
20. I. Dobbie: Resolution and Sampling in Digital Imaging *Microscopy Today.* **15**(3), 24 (2007).
21. J.A. DeRose and M. Doppler: Guidelines for Understanding Magnification in the Modern Digital Microscope Era *Microscopy Today.* **26**(4), 20 (2018).
22. B.M. Patterson, J.P. Escobedo-Diaz, D. Dennis-Koller and E. Cerreta: Dimensional Quantification of Embedded Voids or Objects in Three Dimensions Using X-Ray Tomography *Microscopy and Microanalysis.* **18**(02), 390 (2012).
23. J.D. Stempien, M.A. Plummer, J.L. Schulthess and P.A. Demkowicz: Measurement of Kernel Swelling and Buffer Densification in Irradiated AGR-2 UCO and UO_2 TRISO Fuels. In Proceedings of the 10th International Topical Meeting on High Temperature Reactor Technology, Jun 2-5 2021.
24. Student: The Probable Error of a Mean *Biometrika.* **6**(1), 1 (1908).
25. W.F. Skerjanc and P.A. Demkowicz: PARFUME Theory and Model Basis Report. https://doi.org/10.2172/1471713 Accessed 30 Aug 2021.